J|A|C|S
ARTICLES
Published on Web 05/08/2007

Fluorescence Probe of Trp-Cage Protein Conformation in Solution and in Gas Phase

Anthony T. Iavarone,[†,||] Alexandra Patriksson,[‡] David van der Spoel,[‡] and Joel H. Parks*,[†]

Contribution from the Rowland Institute at Harvard, 100 Edwin H. Land Boulevard, Cambridge, Massachusetts 02142, and Department of Cell and Molecular Biology, Uppsala University, Husargatan 3, Box 596, SE-751 24 Uppsala, Sweden

Received July 17, 2006; E-mail: parks@rowland.harvard.edu

Abstract: Measurements of protein unfolding in the absence of solvent, when combined with unfolding studies in solution, offer a unique opportunity to measure the effects of solvent on protein structure and dynamics. The experiments presented here rely on the fluorescence of an attached dye to probe the local conformational dynamics through interactions with a Trp residue and fields originating on charge sites. We present fluorescence measurements of thermal fluctuations accompanying conformational change of a miniprotein, Trp-cage, in solution and in gas phase. Molecular dynamics (MD) simulations are performed as a function of temperature, charge state, and charge location to elucidate the dye-protein conformational dynamics leading to the changes in measured fluorescence. The results indicate that the stability of the unsolvated protein is dominated by hydrogen bonds. Substituting asparagine for aspartic acid at position 9 results in a dramatic alteration of the solution unfolding curve, indicating that the salt bridge involving Lys8, Asp9, and Arg16 (+ − +) is essential for Trp-cage stability in solution. In contrast, this substitution results in minor changes in the unfolding curve of the unsolvated protein, showing that hydrogen bonds are the major contributor to the stability of Trp-cage in gas phase. Consistent with this hypothesis, the decrease in the number of hydrogen bonds with increasing temperature indicated by MD simulations agrees reasonably well with the experimentally derived enthalpies of conformational change. The simulation results display relatively compact conformations compared with NMR structures that are generally consistent with experimental results. The measured unfolding curves of unsolvated Trp-cage ions are invariant with the acetonitrile content of the solution from which they are formed, possibly as a result of conformational relaxation during or after desolvation. This work demonstrates the power of combined solution and gas-phase studies and of single-point mutations to identify specific noncovalent interactions which contribute to protein-fold stability. The combination of experiment and simulation is particularly useful because these approaches yield complementary information which can be used to deduce the details of structural changes of proteins in the gas phase.

Introduction

The native structures of proteins play a vital role in determining their specific biological functions and interactions with other molecules. One key objective of the life sciences is to understand how the primary sequence encodes the native structure and the dynamics of folding and unfolding processes.[1] Measurements of proteins and peptides in the gas phase[2−4] which complement condensed-phase measurements can help elucidate the role of the solvent environment in producing the native structure and dynamics. The gas-phase measurements are made possible by electrospray ionization (ESI)[5] and matrix-assisted laser desorption ionization[6] which can transfer large molecules into the gas phase without fragmentation. Several methods have been used to study large-scale conformational changes in unsolvated protein and peptide ions such as ion mobility spectroscopy,[7−15]

[†] Rowland Institute at Harvard.
[‡] Uppsala University.
[||] Current address: QB3/Chemistry Mass Spectrometry Facility, University of California, Berkeley, CA 94720-1460.

(1) Fersht, A. *Structure and Mechanism in Protein Science: A Guide to Enzyme Catalysis and Protein Folding*; W. H. Freeman: New York, 1999.
(2) Hoaglund-Hyzer, C. S.; Counterman, A. E.; Clemmer, D. E. *Chem. Rev.* **1999**, *99*, 3037−3079.
(3) Jarrold, M. F. *Annu. Rev. Phys. Chem.* **2000**, *51*, 179−207.
(4) Kaltashov, I. A.; Eyles, S. J. *Mass Spectrometry in Biophysics: Conformation and Dynamics of Biomolecules*; Wiley: Hoboken, 2005.
(5) Fenn, J. B.; Mann, M.; Meng, C. K.; Wong, S. F.; Whitehouse, C. M. *Science* **1989**, *246*, 64−71.
(6) (a) Tanaka, K.; Waki, H.; Ido, Y.; Akita, S. *Rapid Commun. Mass Spectrom.* **1989**, *3*, 436−439. (b) Hillenkamp, F.; Karas, M.; Beavis, R. C.; Chait, B. T. *Anal. Chem.* **1991**, *63*, A1193−A1202.
(7) Wyttenbach, T.; von Helden, G.; Bowers, M. T. *J. Am. Chem. Soc.* **1996**, *118*, 8355−8364.
(8) Li, J.; Taraszka, J. A.; Counterman, A. E.; Clemmer, D. E. *Int. J. Mass Spectrom.* **1999**, *185/186/187*, 37−47.
(9) Kinnear, B. S.; Hartings, M. R.; Jarrold, M. F. *J. Am. Chem. Soc.* **2001**, *123*, 5660−5667.
(10) Badman, E. R.; Hoaglund-Hyzer, C. S.; Clemmer, D. E. *Anal. Chem.* **2001**, *73*, 6000−6007.
(11) Mao, D.; Babu, K. R.; Chen, Y.-L.; Douglas, D. J. *Anal. Chem.* **2003**, *75*, 1325−1330.
(12) Kaleta, D. T.; Jarrold, M. F. *J. Am. Chem. Soc.* **2003**, *125*, 7186−7187.
(13) Counterman, A. E.; Clemmer, D. E. *J. Phys. Chem. B* **2004**, *108*, 4885−4898.
(14) Badman, E. R.; Myung, S.; Clemmer, D. E. *J. Am. Soc. Mass Spectrom.* **2005**, *16*, 1493−1497.

 10.1021/ja065092s CCC: $37.00

ion−molecule reactions,[11,16−18] blackbody infrared radiative dissociation (BIRD),[19,20] electron capture dissociation (ECD),[21−24] and infrared photodissociation spectroscopy.[24,25] Recently, we demonstrated a fluorescence-based probe of conformational dynamics in unsolvated protein and peptide ions that is sensitive to the local molecular environment of the fluorophore.[26,27] This experiment is based on modulation of the fluorescence of an attached fluorescent dye through intramolecular quenching by tryptophan (Trp). This methodology is well-established as a probe of conformational dynamics in solution[28−37] but previously had not been employed in the gas phase. Fluorescence quenching is uniquely sensitive to Ångström-scale fluctuations in the fluorophore-quencher distance[33] and has been used to probe the interconversion between conformers in single molecules.[35]

Our initial study[26] demonstrated the use of fluorescence to follow conformational change occurring with increasing temperature in unsolvated ions of Trp-cage, a 20-residue miniprotein. The sequence is a construct resulting from truncation and mutation of a 39-residue peptide, exendin-4, derived from Gila monster saliva, and has been shown to be fully structured in aqueous solution at low temperatures.[38] The folded structure has a compact hydrophobic core consisting of a Trp side chain which is "caged" by several hydrophobic residues. The NMR structure of the Trp-cage also indicates a salt bridge between the negatively charged aspartic acid (Asp) at position 9 and the positively charged lysine (Lys) and arginine (Arg) at positions 8 and 16, respectively.[38] Trp-cage is remarkable in that it is the smallest example of a protein with cooperatively folded tertiary structure in aqueous solution[38,39] and that it folds in only four microseconds.[40] Miniproteins such as Trp-cage are useful tools for the study of protein folding because their small size makes them amenable to chemical synthesis which expedites the production of variants for mutational studies.[38,39] In addition, they are readily tractable by molecular dynamics (MD) simulations.[41−47] Here, we report fluorescence measurements of Trp-cage as a function of temperature in solution and in gas phase, examining the roles of charge state, dye and charge locations, and solvent composition. We also present measurements of a variant Trp-cage in which Asp9 has been replaced by asparagine (Asn) to determine the importance of the salt bridge in stabilizing the folded structure both in solution and in gas phase. Our experiments are complemented by MD simulations performed as a function of charge state, charge location, and temperature to elucidate the atomic-level details of the dye-protein conformational dynamics leading to the observed changes in fluorescence.

Methods and Analysis

Materials. Derivatized peptides were synthesized by BioMer Technology (Hayward, CA) and purified by reversed-phase HPLC to a stated purity of >70% prior to shipment. The BODIPY analogues of tetramethylrhodamine and Texas Red, "BoTMR" and "BoTR", respectively, were obtained from Invitrogen (Carlsbad, CA). The chemical structures and excitation and emission spectra of these dyes have been published elsewhere.[48,49] The amino acid sequences are (BoTR)-NLYIQWLKDGGPSSGRPPPSK-$CONH_2$, NLYIQWLKDGGPSSGRPPPSK(BoTMR)-$CONH_2$, and NLYIQWLKNGGPSSGRPPPSK(BoTMR)-$CONH_2$ and are referred to herein as "BoTR-Trp-cage", "Trp-cage-BoTMR", and "D9N Trp-cage-BoTMR", respectively. The amino acid sequence is the same as that of Trp-cage with the addition of lysine at the C-terminus to allow for the conjugation of a dye (via the ϵ-amine). Attachment of the dyes does not significantly alter the emission or excitation spectra (data not shown). Ammonium acetate (>98%) was obtained from Sigma (St. Louis, MO), and acetonitrile (>99.9%), ammonium bicarbonate (>99%), and distilled, deionized water were obtained from Fisher Scientific (Fair Lawn, NJ), Mallinckrodt (Hazelwood, MO), and VWR (West Chester, PA), respectively. Electrospray solutions contain 10^{-5} M analyte in aqueous or 1:1 acetonitrile/water solutions. Ammonium bicarbonate and acetate (10^{-2} M) are added for pH stabilization.

Mass Spectrometry. The instrumentation used for these experiments is described elsewhere.[27] Briefly, measurements are performed using a quadrupole ion trap mass spectrometer that was designed and built in-house.[50] Droplets and ions formed by nanoelectrospray (nanoES)[51] are sampled from atmospheric pressure through a stainless steel capillary maintained at 333 K and transferred into a quadrupole ion trap which can be heated to temperatures as high as ~443 K. The use of higher trap temperatures results in ion fragmentation >2%. The ions of interest

(15) Sudha, R.; Kohtani, M.; Jarrold, M. F. *J. Phys. Chem. B* **2005**, *109*, 6442−6447.
(16) Green, M. K.; Lebrilla, C. B. *Mass Spectrom. Rev.* **1997**, *16*, 53−71.
(17) Suckau, D.; Shi, Y.; Beu, S. C.; Senko, M. W.; Quinn, J. P.; Wampler, F. M., III; McLafferty, F. W. *Proc. Natl. Acad. Sci. U.S.A.* **1993**, *90*, 790−793.
(18) Gross, D. S.; Schnier, P. D.; Rodriguez-Cruz, S. E.; Fagerquist, C. K.; Williams, E. R. *Proc. Natl. Acad. Sci. U.S.A.* **1996**, *93*, 3143−3148.
(19) (a) Dunbar, R. C. *Mass Spectrom. Rev.* **2004**, *23*, 127−158. (b) Price, W. D.; Schnier, P. D.; Williams, E. R. *Anal. Chem.* **1996**, *68*, 859−866.
(20) Gross, D. S.; Zhao, Y.; Williams, E. R. *J. Am. Soc. Mass Spectrom.* **1997**, *8*, 519−524.
(21) Breuker, K.; Oh, H.; Horn, D. M.; Cerda, B. A.; McLafferty, F. W. *J. Am. Chem. Soc.* **2002**, *124*, 6407−6420.
(22) Adams, C. M.; Kjeldsen, F.; Zubarev, R. A.; Budnik, B. A.; Haselmann, K. F. *J. Am. Soc. Mass Spectrom.* **2004**, *15*, 1087−1098.
(23) Polfer, N. C.; Haselmann, K. F.; Langridge-Smith, P. R. R.; Barran, P. E. *Mol. Phys.* **2005**, *103*, 1481−1489.
(24) Oh, H.; Breuker, K.; Sze, S. K.; Ge, Y.; Carpenter, B. K.; McLafferty, F. W. *Proc. Natl. Acad. Sci. U.S.A.* **2002**, *99*, 15863−15868.
(25) Oomens, J.; Polfer, N.; Moore, D. T.; van der Meer, L.; Marshall, A. G.; Eyler, J. R.; Meijer, G.; von Helden, G. *Phys. Chem. Chem. Phys.* **2005**, *7*, 1345−1348.
(26) Iavarone, A. T.; Parks, J. H. *J. Am. Chem. Soc.* **2005**, *127*, 8606−8607.
(27) Iavarone, A. T.; Meinen, J.; Schulze, S.; Parks, J. H. *Int. J. Mass Spectrom.* **2006**, *253*, 172−180.
(28) Lapidus, L. J.; Eaton, W. A.; Hofrichter, J. *Proc. Natl. Acad. Sci. U.S.A.* **2000**, *97*, 7220−7225.
(29) (a) Thompson, P. A.; Muñoz, V.; Jas, G. S.; Henry, E. R.; Eaton, W. A.; Hofrichter, J. *J. Phys. Chem. B* **2000**, *104*, 378−389. (b) Jas, G. S.; Eaton, W. A.; Hofrichter, J. *J. Phys. Chem. B* **2001**, *105*, 261−272.
(30) Hagen, S. J.; Carswell, C. W.; Sjolander, E. M. *J. Mol. Biol.* **2001**, *305*, 1161−1171.
(31) Hudgins, R. R.; Huang, F.; Gramlich, G.; Nau, W. M. *J. Am. Chem. Soc.* **2002**, *124*, 556−564.
(32) Marmé, N.; Knemeyer, J.-P.; Sauer, M.; Wolfrum, J. *Bioconjugate Chem.* **2003**, *14*, 1133−1139.
(33) (a) Neuweiler, H.; Schulz, A.; Böhmer, M.; Enderlein, J.; Sauer, M. *J. Am. Chem. Soc.* **2003**, *125*, 5324−5330. (b) Doose, S.; Neuweiler, H.; Sauer, M. *Chem. Phys. Chem.* **2005**, *6*, 2277−2285. (c) Neuweiler, H.; Doose, S.; Sauer, M. *Proc. Natl. Acad. Sci. U.S.A.* **2005**, *102*, 16650−16655.
(34) Vaiana, A. C.; Neuweiler, H.; Schulz, A.; Wolfrum, J.; Sauer, M.; Smith, J. C. *J. Am. Chem. Soc.* **2003**, *125*, 14564−14572.
(35) Yang, H.; Luo, G.; Karnchanaphanurach, P.; Louie, T.-M.; Rech, I.; Cova, S.; Xun, L.; Xie, X. S. *Science* **2003**, *302*, 262−266.
(36) Jones, G., II; Zhou, X.; Vullev, V. I. *Photochem. Photobiol. Sci.* **2003**, *2*, 1080−1087.
(37) Huang, F.; Hudgins, R. R.; Nau, W. M. *J. Am. Chem. Soc.* **2004**, *126*, 16665−16675.
(38) Neidigh, J. W.; Fesinmeyer, R. M.; Andersen, N. H. *Nat. Struct. Biol.* **2002**, *9*, 425−430.
(39) Gellman, S. H.; Woolfson, D. N. *Nat. Struct. Biol.* **2002**, *9*, 408−410.
(40) Qiu, L.; Pabit, S. A.; Roitberg, A. E.; Hagen, S. J. *J. Am. Chem. Soc.* **2002**, *124*, 12952−12953.
(41) Simmerling, C.; Strockbine, B.; Roitberg, A. E. *J. Am. Chem. Soc.* **2002**, *124*, 11258−11259.
(42) Snow, C. D.; Zagrovic, B.; Pande, V. S. *J. Am. Chem. Soc.* **2002**, *124*, 14548−14549.
(43) Pitera, J. W.; Swope, W. *Proc. Natl. Acad. Sci. U.S.A.* **2003**, *100*, 7587−7592.
(44) Chowdhury, S.; Lee, M. C.; Xiong, G. M.; Duan, Y. *J. Mol. Biol.* **2003**, *327*, 711−717.
(45) Zhou, R. *Proc. Natl. Acad. Sci. U.S.A.* **2003**, *100*, 13280−13285.
(46) Seshasayee, A. S. N. *Theor. Biol. Med. Modell.* **2005**, *2*, 7.
(47) Ding, F.; Buldyrev, S. V.; Dokholyan, N. V. *Biophys. J.* **2005**, *88*, 147−155.
(48) Molecular Probes. http://probes.invitrogen.com (accessed 2006).
(49) Danell, A. S.; Parks, J. H. *Int. J. Mass Spectrom.* **2003**, *229*, 35−45.

are isolated using RF ramping and SWIFT ejection. The background helium gas pressure is $\sim 3 \times 10^{-6}$ Torr and is pulsed to $\sim 2 \times 10^{-4}$ Torr for ion loading and thermalization. (The pressure within the trap is ca. 30−35-fold higher owing to the low conductance of the trap apertures.) Approximately 2000 (±15%) ions are loaded and thermalized in the trap for 1 s before measuring fluorescence at $q_z = 0.50$. The trapped ions undergo $>10^5$ collisions which equilibrate them with the bath gas which is maintained at the temperature of the trap. After the fluorescence measurement the ions are ejected from the trap and detected by an electron multiplier.

Gas-Phase Fluorescence. The ions of interest are irradiated with 532 nm light from a continuous wave Nd:YAG laser (Millennia VIs, Spectra-Physics, Irvine, CA) for 100 ms at an intensity of 132 W/cm^2. The Gaussian laser beam diameter is ~220 μm to minimize scattering of the light on the trap apertures. The laser-ion cloud overlap is optimized by alignment of the laser and by adjustment of the DC bias applied to the trap endcaps which alters the cloud position. A two-channel detection system isolates and quantifies BoTMR and BoTR fluorescence. Twenty-five replicate measurements are performed for each data point, and each set of measurements is performed at least two times on different days. The day-to-day reproducibility of absolute intensity is within ±20%. The fluorescence data routinely exhibit a signal-to-noise (S/N) ratio of ~400 and this offers several distinct experimental advantages. High quality fluorescence can be collected from relatively few molecules (<200) in a small volume of the trapped ion cloud ($\sim 2 \times 10^{-5}$ cm^3) which can be efficiently focused onto the detector. Trapping small numbers of molecular ions minimizes space−charge interactions resulting in smaller ion clouds and more reliable simulations of ion trajectories. Moreover, it should be possible to decrease the number of irradiated ions to ≤10 to reduce the effects of ensemble averaging and in particular to perform fluorescence correlation spectroscopy.[52]

Various fluorescent dyes were screened to identify those which would not significantly change their radiative properties upon desolvation and heating. BoTMR and BoTR were selected because they are uncharged in solution, excited efficiently at 532 nm, and emit fluorescence with high quantum yield (>80%). In addition, their absorption and emission spectra exhibit minimal solvent and temperature dependence.[49] Perhaps of highest significance is that the high fluorescence S/N obtained with BoTMR and BoTR allows for excitation using low laser intensities which minimizes heating of the gas-phase biomolecules. In the present experiments, fluorescence measurements estimate that the laser-induced temperature increase of trapped Trp-cage ions in the presence of the helium background gas is less than 2 K for an intensity of 132 W/cm^2. Clearly, the laser-induced heating of the ions becomes more severe if the fluorescence probe relies on a natural fluorophore such as Trp which has small quantum yield (~20%).[53]

Solution-Phase Spectroscopy. Fluorescence emission and excitation spectra are measured on a model J-810 spectrometer (Jasco, Easton, MD). The excitation wavelength of intrinsic Trp fluorescence is 268 nm and the excitation and emission bandwidths are both 10 nm. Solutions are contained in quartz cuvettes (Spectrocell, Oreland, PA) with screw caps to prevent evaporation. The sample temperature is regulated with a precision of ±0.5 K by a Peltier device. For measuring BoTMR/BoTR and intrinsic Trp fluorescence the solutions contain 3×10^{-7} and 10^{-5} M analyte, respectively, in water or 1:1 acetonitrile/water.

Gas-Phase Fluorescence Model. Measurements in solution were performed to characterize the quenching of BoTMR fluorescence through bimolecular interactions with Trp and also the intramolecular quenching occurring in Trp-cage-BoTMR. These measurements[54] indicate that the dominant process is dynamic quenching of the dye excited-state rather than formation of a nonradiative complex. Cyclic voltammetry measurements[54] indicate that the quenching process in solution is dominated by electron transfer. Considering these results, we assume the quenching in gas phase occurs via a local interaction between the excited dye and Trp. As a result, the quenching process is sensitive to conformational changes which alter the Trp position. This requires a sufficiently high dye-Trp contact rate[28,30,33,37] to ensure the likelihood of quenching during a radiative lifetime of 10 ns. A rough upper bound of the gas-phase quenching rate can be estimated by considering the rate of contact between the Trp residue and the dye tethered to the protein by an aminohexanoate linker. In gas phase the contact rate will not be constrained by diffusion-limited kinetics and can be estimated by considering the dye to be freely moving within a volume determined by the tether length R. The contact rate can be estimated by $k_c \approx n\nu\sigma$ in which n is the density associated with the tethered BoTMR, $n \approx 1/V = (4\pi R^3/3)^{-1}$. Here R is the distance from the center of mass of the dye linked to the polypeptide by the tether ($R \approx 12$ Å). An upper bound for the collision rate of $k_c \approx 2 \times 10^{10}$ s^{-1} is obtained for a thermal relative velocity, $\nu \approx 1.4 \times 10^4$ cm/s, and a hard sphere collision cross-section estimated to be $\sigma \approx 1 \times 10^{-14}$ cm^2. This value for the contact rate should be considered an upper bound since it assumes free access to a Trp residue having a dye-Trp separation within the tethered volume, and the excluded volume is neglected. Here, quenching is assumed to occur on contact. However, even if the contact rate were a factor of 10 lower, it would still be sufficient to quench the excited-state at a rate greater than the radiative rate.[54]

A model expressing the temperature dependence of the fluorescence quenching in the gas phase was derived assuming the two-state character[40] of Trp-cage is retained. This model assumes that the Trp becomes increasingly accessible to interaction with the dye as the fraction of unfolded proteins in the ensemble increases. In contrast to a model used previously to describe Trp fluorescence during peptide unfolding,[29] the present model assumes that quenching is absent in the folded state and occurs with a rate constant, k_q, in the unfolded state:

$$I \propto \phi = \chi_f + \frac{1}{1 + k_q\tau_0}\chi_u \qquad (1)$$

The fluorescence intensity, I, is proportional to the quantum yield at a given temperature, ϕ. χ_f and χ_u are the protein fractions in the folded and unfolded states, respectively, where $\chi_f = [1 + \exp(-\Delta G/kT)]^{-1}$ and $\chi_u = 1 - \chi_f$. Fits of the data to this model yield the thermochemical parameters associated with the conformational change. The resulting fits display an insensitivity to different models used to estimate k_q because in each case it is found that $k_q\tau_0 \gg 1$, a consequence of the gas-phase kinetics.

The relatively simple model presented here assumes that Trp quenching is the primary mechanism for changes in fluorescence. In previous fluorescence measurements on peptides,[27] it was observed that changes in fluorescence can also result from interactions of the dye with Coulomb fields. These fields can induce a change in the dye absorption strength and also a shift in the absorption spectrum. The importance of these field effects is currently under investigation and will be the subject of future experiments.

Coulomb Energy. The effects of Coulomb repulsion on conformational change of unsolvated, multiply charged proteins are estimated as follows. For a molecule, M, with n positive charges, which undergoes an unfolding process,

$$M_{fold}^{n+} \rightarrow M_{unf}^{n+} \qquad (2)$$

(50) Khoury, J. T.; Rodriguez-Cruz, S. E.; Parks, J. H. *J. Am. Soc. Mass Spectrom.* **2002**, *13*, 696−708.
(51) Wilm, M.; Mann, M. *Anal. Chem.* **1996**, *68*, 1−8.
(52) Hess, S. T.; Huang, S.; Heikal, A. A.; Webb, W. W. *Biochemistry* **2002**, *41*, 697−705.
(53) Creighton, T. E. *Proteins: Structures and Molecular Properties*, 2nd Ed.; W. H. Freeman: New York, 1993.
(54) Unpublished data.

the Coulomb energy released due to an increase in separation between like charges, ΔE_{Coul}, is the difference between the Coulomb energies of the final (unfolded) and initial (folded) states.

$$\Delta E_{Coul} = E_{unf} - E_{fold} < 0 \quad (3)$$

E_{fold} and E_{unf} are approximated by summing the pairwise interactions between point charges in the folded and unfolded states, respectively (dielectric polarizability = 1.3).[55] The distances between the charge sites in the folded and unfolded states are derived from MD simulations performed at 302 and 445 K, respectively. The measured enthalpy change, ΔH, is the sum of the intrinsic enthalpy of unfolding, ΔH_{int}, and ΔE_{Coul}. Thus, ΔH_{int} is the experimentally derived ΔH minus the calculated ΔE_{Coul}.

$$\Delta H_{int} = \Delta H - \Delta E_{Coul} \quad (4)$$

Molecular Dynamics. The molecular dynamics simulations of Trp-cage are performed using the GROMACS software package[56,57] with the OPLS/AA force field.[58] The conformation determined by NMR[38] is used as the initial structure. To match the molecule used for experiments, an amidated lysine residue was attached to the C-terminus, and the BODIPY dye was attached to the side-chain nitrogen of Lys21. Force field parameters for the dye were taken as much as possible from analogues (similar chemical groups) available in the OPLS/AA force field. For the ring system a quantum chemical calculation was performed using the Gaussian 2003 software[59] at the Hartree−Fock level with the 6-31G** basis set. For the boron atom no ready Lennard-Jones parameters are available in the force field, but since the atom is at the center of a tetrahedral arrangement of atoms, the exact parameters are not crucial and the parameters for carbon were used instead. The charges, which were determined from a Merz−Kollman population analysis,[60] and the Lennard-Jones parameters for B, F, and N atoms in the dye are given in the Supporting Information. Torsional potentials were added to keep the ring system flat, with the same parameters as those used for the Trp side chain in the OPLS/AA force field. Both complete molecules were subject to energy minimization using the limited-memory Broyden−Fletcher−Goldfarb−Shanno algorithm[61] with position restraints on the non-hydrogen atoms in the original Trp-cage (residues 1−20). Subsequently 10 ns MD simulations were done with position restraints (force constant 1000 kJ/mol·nm^2) on the protein atoms (except hydrogens), allowing the dye to relax without affecting the conformation of the protein.

Charge locations for these simulations on Trp-cage ions have been assigned to examine the effects of charge location on the simulated structure and dynamics. Specifically, simulations were performed and compared with fluorescence data to determine whether Gln5 or Lys8 was the preferred protonation site. In the first case, charges were located on the basis of intrinsic gas-phase basicity (GB). Since the GB of Lys is 51 kJ/mol higher than that of Gln,[62] the two charge states, 2+ and 3+, were generated with Lys8 and Arg16 protonated in the 2+ ion, and in the 3+ ion the third charge location is the N-terminus. In the second case, charges were located consistent with recent ECD measurements of the 2+ and 3+ ions of Trp-cage reported by Zubarev and co-workers.[22,63] In this second case the two charge states, 2+ and 3+, were generated with Gln5 and Arg16 protonated in the 2+ ion, and in the 3+ ion the third charge location is the N-terminus.

Replica exchange MD (REMD) simulations[64] of 500 ns were performed at 16 different temperatures, namely at 280, 284, 289, 295, 302, 310, 319, 329, 340, 352, 365, 379, 394, 410, 427, and 445 K, respectively. Both the 2+ and the 3+ ions were simulated in the same fashion. No cutoff is used for Coulomb and Van der Waals interactions because all interactions are explicitly calculated in vacuo. In the REMD simulations the temperature was controlled using the Berendsen weak coupling algorithm[65] with a time constant of 0.1 ps. The LINCS algorithm[66] was used for constraining the bond lengths, allowing for an integration time step of 2 fs. Exchanges were attempted every ps and the exchange probability varied between 86% at the lowest and 53% at the highest temperature.

The total number of hydrogen bonds between all of the backbone carbonyl oxygens and any other part of the molecule at a given temperature is calculated by summing the fractions of instances the carbonyl oxygens are found to be participating in hydrogen bonds during the simulation. The total number of instances is 250000 (one for every other ps in the REMD simulations). Hydrogen bonds are defined using a geometric criterion where the distance between donor and acceptor is less than 0.35 nm and the hydrogen donor−acceptor angle should be less than 30 degrees.

Results

Ions Formed by nanoES. The charge state distributions of Trp-cage-BoTMR formed under optimum conditions for the 2+ and 3+ charge states are shown in Figure 1panels a and c, respectively. (The DC voltage applied to the sampling capillary was 230 and 150 V, respectively.) An ion of interest such as the 2+ or 3+ charge state is isolated by ejecting the other ions from the trap (Figure 1 panels b and d, respectively) prior to measuring fluorescence. As shown in Figure 1, the mass spectral resolution is sufficient to positively identify the intact, unsolvated ions.

Fluorescence Measurements. Fluorescence measurements of gas-phase ions were performed at 20 K increments between 303 and 423 K and at 438 K. For the 2+ ions of Trp-cage-BoTMR the fluorescence is essentially unchanged between 303 and 403 K. The fluorescence then decreases by ∼30% as the temperature is further increased to 438 K (Figure 2a). In contrast, for the 3+ ions the fluorescence is constant from 303 to 363 K, but then decreases by ∼75% upon further heating to 438 K (Figure 2b). For both the 2+ and 3+ ions the changes in fluorescence as a function of temperature are invariant with electrospray solvent composition (aqueous or 1:1 acetonitrile/water). As noted previously,[26] the fluorescence of singly charged, positive ions of BODIPY TMR dye is constant over the same temperature range (data not shown), indicating that the changes in fluorescence shown in Figure 2 are due to the dynamics of the polypeptide and not the intrinsic photophysics of the dye. Measurements were also made of the 3+ ions of BoTR-Trp-cage, in which the dye is attached to the N-terminus

(55) Schnier, P. D.; Gross, D. S.; Williams, E. R. *J. Am. Chem. Soc.* **1995**, *117*, 6747−6757.
(56) Lindahl, E.; Hess, B.; Van der Spoel, D. *J. Mol. Mod.* **2001**, *7*, 306−317.
(57) Van der Spoel, D.; Lindahl, E.; Hess, B.; Groenhof, G.; Mark, A. E.; Berendsen, H. J. C. *J. Comp. Chem.* **2005**, *26*, 1701−1718.
(58) Jorgensen, W. L.; Maxwell, D. S.; Tirado-Rives, J. *J. Am. Chem. Soc.* **1996**, *118*, 11225−11236.
(59) Frisch, M. J.; et al. *Gaussian 03*, revision C.02; Gaussian, Inc.: Wallingford, CT, 2004.
(60) Besler, B. H.; Merz, K. M., Jr.; Kollman, P. A. *J. Comp. Chem.* **1990**, *11*, 431−439.
(61) Byrd, R. H.; Lu, P. H.; Nocedal, J.; Zhu, C. Y. *SIAM J. Sci. Stat. Comput.* **1995**, *16*, 1190−1208.
(62) Hunter, E. P.; Lias, S. G. In *NIST Chemistry Webbook*; Mallard, W. G., Lindstrom, P. J., Eds.; NIST Standard Reference Database Number 69; National Institute of Standards and Technology: Gaithersburg, MD, March 1998.
(63) (a) Patriksson, A.; Adams, C.; Kjeldsen, F.; Raber, J.; Van der Spoel, D.; Zubarev, R. A. *Int. J. Mass Spectrom.* **2005**, *248*, 124−135. (b) Adams, C. M.; Kjeldsen, F.; Patriksson, A.; Van der Spoel, D.; Gräslund, A.; Papadopoulos, E.; Zubarev, R. A. *Int. J. Mass Spectrom.* **2006**, *253*, 263−273.
(64) Hukushima, K.; Nemoto, K. *J. Phys. Soc. Jpn.* **1996**, *65*, 1604−1608.
(65) Berendsen, H. J. C.; Postma, J. P. M.; Vangusteren, W. F.; DiNola, A.; Haak, J. R. *J. Chem. Phys.* **1984**, *81*, 3684−3690.
(66) Hess, B.; Bekker, H.; Berendsen, H. J. C.; Fraaije, J. G. E. M. *J. Comp. Chem.* **1997**, *18*, 1463−1472.

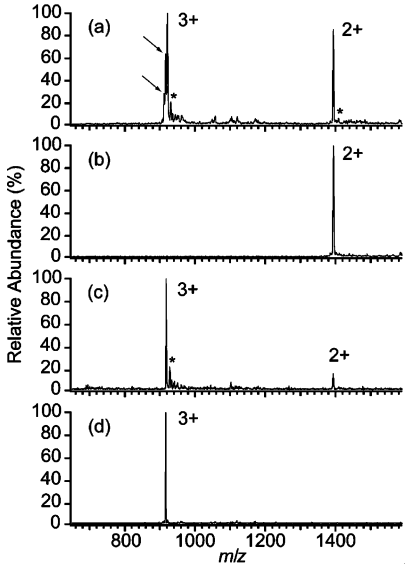

Figure 1. Representative mass spectra of Trp-cage-BoTMR: (a) charge-state distribution in which the abundance of the 2+ ion is optimized; (b) isolation spectrum of the 2+ ion; (c) charge-state distribution in which the abundance of the 3+ is optimized; (d) isolation spectrum of the 3+ ion. The arrows in panel a denote peaks corresponding to neutral losses of ~17 or 18 Da, presumably molecules of water and/or ammonia, from the 3+ ion. The asterisks in panels a and c denote peaks corresponding to an addition of ~30 Da.

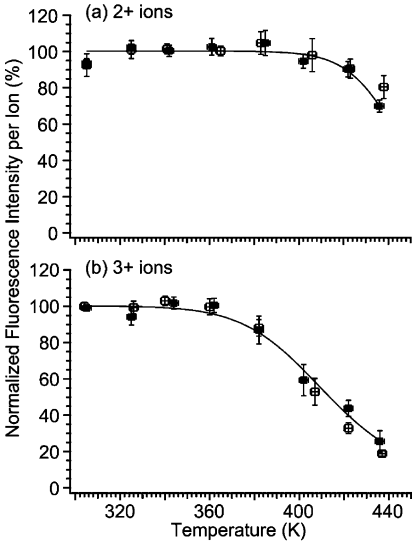

Figure 2. Normalized fluorescence intensity per ion vs temperature for (a) 2+ and (b) 3+ ions of Trp-cage-BoTMR. Data points for ions formed from aqueous and 1:1 acetonitrile/water solutions are denoted by closed and open square markers, respectively. Model fits to the data are delineated by curves. Intensities are normalized to 303 K values.

instead of the C-terminus, to examine the effects of changing the dye location. The resulting fluorescence data (shown in the Supporting Information) are very similar to those of Trp-cage-BoTMR.

The enthalpy changes, ΔH, derived from model fits to the data for the 2+ and 3+ ions of Trp-cage-BoTMR formed from the aqueous solution are 182% and 52%, respectively, larger than those measured in aqueous solution, and the entropy changes, ΔS, for these charge states are 98% and 16%, respectively, larger than those in solution (Table 1). Increasing the acetonitrile content of the aqueous electrospray solution from 0% to 50% has no significant effect on the measured melting curves (Figure 2) or thermochemical parameters (Table 1) of the gas-phase ions. In contrast, the melting temperature, T_m, *in solution* is 32 K lower in 50% acetonitrile than in the aqueous solution with 0% acetonitrile (Figure 3).

Aspartic Acid/Asparagine Substitution. Heating an aqueous solution of Trp-cage-BoTMR between 273 and 353 K results in a sigmoidal 212% increase in the intrinsic Trp fluorescence (peak emission wavelength $\approx$ 350 nm) which indicates an unfolding transition with $T_m = 323$ K (Figure 4, closed squares). In contrast, repeating this measurement using the variant D9N Trp-cage-BoTMR, in which Asp9 has been replaced by Asn, results in a gradual 50% *decrease* in the Trp fluorescence (Figure 4, open squares). This indicates that the single mutation, D9N, dramatically disrupts the stability of the folded structure in aqueous solution. In the gas phase, the absolute fluorescence intensities per ion of the 2+ and 3+ charge states of the D9N variant are 12 (±5)% and 29 (±4)% lower, respectively, than those of the corresponding ions of Trp-cage-BoTMR at 303 K (data not shown). The lower intensity of the D9N mutant is consistent with more efficient quenching in a structure in which the Trp side chain is more accessible to contact with the dye. As the temperature is increased from 303 to 438 K, the decrease in fluorescence is slightly greater for ions of D9N Trp-cage-BoTMR than for corresponding ions of Trp-cage-BoTMR (Figure 5) and the associated enthalpy and entropy changes are not significantly different (Table 2). Thus, in contrast to the results obtained in solution, replacing Asp9 with Asn does not appear to significantly alter the stability of the gas-phase protein structure.

Discussion

Intramolecular Interactions. The fluorescence intensity of unsolvated Trp-cage ions is essentially constant up to a certain temperature and then decreases as the temperature is further increased. The decrease in fluorescence is consistent with a temperature-induced conformational change which results in a greater exposure of the Trp side chain to quenching interactions with the dye. The greater decrease observed for the 3+ ion (Figure 2b) compared with that of the 2+ ion (Figure 2a) is consistent with a transition that is accelerated by greater Coulomb repulsion in the higher charge state.[67−69] An analysis of the interactions which contribute to the stability of the gas-phase structure follows.

In solution, no distinct melting transition is observed between 273 and 343 K for the D9N mutant (Figure 4). Asp has a carboxylic acid side chain which is negatively charged in solution over a wide pH range (pK = 3.9)[70] but the Asn side chain is the uncharged amide analogue of Asp. Substituting Asn for Asp9 breaks the + − + salt bridge formed between Lys8, Asp9, and Arg16.[38] Apparently, the loss of this interaction results in the dramatic disruption of the Trp-cage fold in solution. (A single solvent-exposed salt bridge can contribute 0.4−2 kJ/mol to protein fold stability in solution.)[1] Andersen and co-workers[38] evaluated several sequences which differed at multiple positions to optimize the Trp-cage stability. The sequences

(67) Clemmer, D. E.; Jarrold, M. F. *J. Mass Spectrom.* **1997**, *32*, 577−592.
(68) Arteca, G. A.; Reimann, C. T.; Tapia, O. *Chem. Phys. Lett.* **2001**, *350*, 277−285.
(69) Schnier, P. D.; Gross, D. S.; Williams, E. R. *J. Am. Soc. Mass Spectrom.* **1995**, *6*, 1086−1097.
(70) Lehninger, A. L. *Biochemistry*, 2nd ed.; Worth: New York, 1975.

Table 1. Thermochemical Parameters Derived from Fluorescence Measurements[a]

analyte	charge state	electrospray solvent	ΔH (kJ/mol)	ΔH_{int}(Q5) (kJ/mol)[b]	ΔH_{int} (K8) (kJ/mol)[c]	ΔS (J/mol·K)
Trp-cage-BoTMR	2+	aqueous	137 ± 52	138 ± 52	139 ± 52	307 ± 120
Trp-cage-BoTMR	2+	1:1 ACN[d]/water	108 ± 57	109 ± 57	110 ± 57	236 ± 132
Trp-cage-BoTMR	3+	aqueous	74 ± 11	146 ± 11	84 ± 11	180 ± 27
Trp-cage-BoTMR	3+	1:1 ACN[d]/water	89 ± 5	161 ± 5	99 ± 5	219 ± 11
BoTR-Trp-cage	3+	aqueous	75 ± 8	147 ± 8	85 ± 8	182 ± 18
(solution)[e]			48.6			155

[a] Stated errors are ± one standard deviation from the mean. [b] Calculated using charge locations Q5 and R16 for the 2+ ion and N1, Q5, and R16 for the 3+ ion. [c] Calculated using charge locations K8 and R16 for the 2+ ion and N1, K8, and R16 for the 3+ ion. [d] ACN = acetonitrile. [e] Literature values (ref 40).

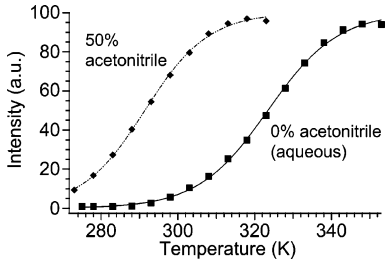

Figure 3. Solution thermal unfolding curves measured by intrinsic Trp fluorescence (268 nm excitation) of Trp-cage-BoTMR (10^{-5} M) in water/acetonitrile solutions in which the volume fraction of acetonitrile is 0% (squares) or 50% (diamonds).

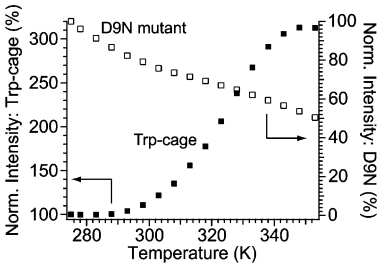

Figure 4. Solution thermal unfolding curves measured by intrinsic Trp fluorescence of Trp-cage-BoTMR (closed squares, left *y*-axis) and D9N mutant (open squares, right *y*-axis) in aqueous solutions.

which had Asn instead of Asp were less well-folded as determined by NMR.[38] To our knowledge, the present work represents the first evaluation of the *single-point* mutation, D9N, of Trp-cage in solution and in gas phase.

The lower fluorescence intensity measured for unsolvated ions of the D9N mutant at 303 K compared with that of unmutated Trp-cage is consistent with some degree of correlation between conformations in solution and in gas phase. The D9N mutant presumably has the Trp side chain less sequestered in its cage, leading to more quenching and lower fluorescence due to increased dye-Trp interaction. Interestingly, the overall shapes of the gas-phase melting curves of Trp-cage and the D9N mutant (Figure 5) are not substantially different, and the associated thermochemical parameters are the same within experimental uncertainty (Table 2). The enthalpy change for the D9N mutant is expected to be significantly lower[71] than that of Trp-cage if a salt bridge involving Asp9 were stabilizing the gas-phase structure of Trp-cage. Thus the salt bridge, though an important contributor to stability in solution, does not appear to be a significant contributor to the observed stability of these gas-phase ions.

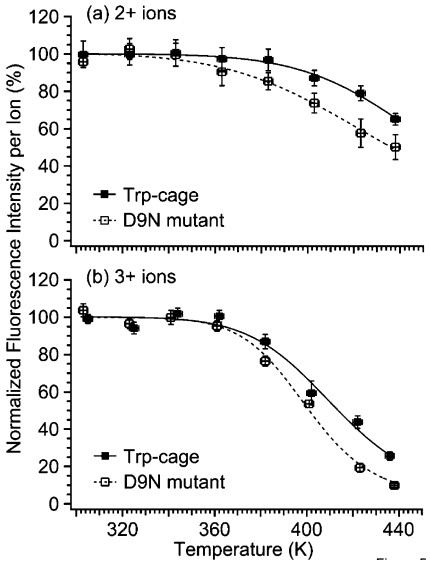

Figure 5. Normalized fluorescence intensity per ion vs temperature for the (a) 2+ and (b) 3+ ions of Trp-cage-BoTMR (closed squares) and D9N Trp-cage-BoTMR (open squares). Model fits to the data are delineated by curves. Intensities are normalized to 303 K values.

Table 2. Differences Between Thermochemical Parameters of Gas-Phase Ions of Trp-cage-BoTMR and the Variant D9N Trp-cage-BoTMR Derived from Fluorescence Measurements

charge state	$\Delta(\Delta H)$ (kJ/mol)	$\Delta(\Delta S)$ (J/mol·K)
2+	16 ± 12	29 ± 30
3+	17 ± 19	44 ± 48

In solution Lys8 is in its protonated, positively charged form and Asp9 is in its negatively charged, deprotonated form. However, in the gas phase, charge separation is destabilized by the lack of solvation,[72] and this may favor a configuration in which Lys8 is deprotonated and Asp9 is protonated, i.e., both residues are uncharged. Evidence has been presented[73−75] which indicates the existence of salt-bridge structures in unsolvated biomolecule ions such as the $(M+H)^+$ of bradykinin. One factor which plays a role in the presence or absence of salt bridges is the gas-phase basicities (GB) of the participating groups.[76,77]

(71) Strittmatter, E. F.; Williams, E. R. *J. Phys. Chem. A* **2000**, *104*, 6069−6076.
(72) Zheng, Y.-J.; Ornstein, R. L. *J. Am. Chem. Soc.* **1996**, *118*, 11237−11243.
(73) Campbell, S.; Rodgers, M. T.; Marzluff, E. M.; Beauchamp, J. L. *J. Am. Chem. Soc.* **1995**, *117*, 12840−12854.
(74) Schnier, P. D.; Price, W. D.; Jockusch, R. A.; Williams, E. R. *J. Am. Chem. Soc.* **1996**, *118*, 7178−7189.
(75) Wyttenbach, T.; Liu, D.; Bowers, M. T. *Int. J. Mass Spectrom.* **2005**, *240*, 221−232.
(76) Strittmatter, E. F.; Wong, R. L.; Williams, E. R. *J. Phys. Chem. A* **2000**, *104*, 10271−10279.
(77) Strittmatter, E. F.; Williams, E. R. *Int. J. Mass Spectrom.* **2001**, *212*, 287−300.

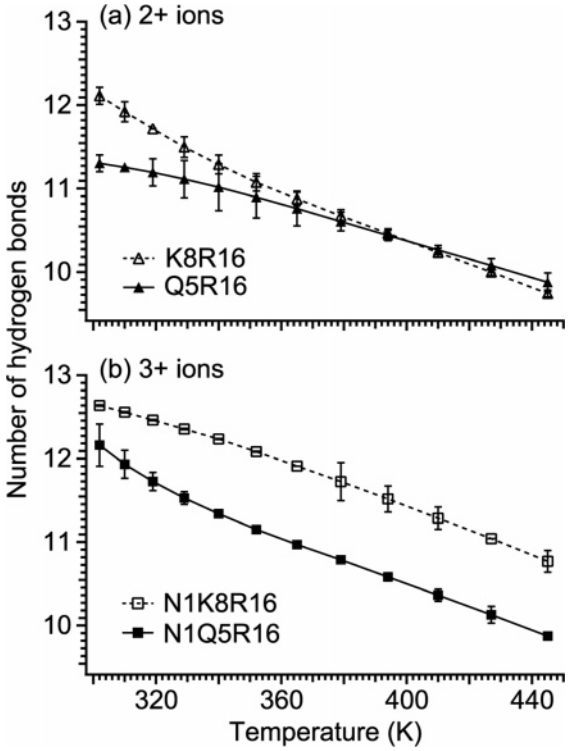

Figure 6. The total number of hydrogen bonds between the backbone carbonyl oxygens and any other part of the molecule for the (a) 2+ (K8R16 charge configuration, open triangles; Q5R16, closed triangles) and (b) 3+ (N1K8R16, open squares; N1Q5R16, closed squares) ions of Trp-cage-BoTMR, as determined from molecular dynamics simulations. The lines connecting the data points are included to guide the eye.

Salt-bridge structures are favored by higher GB,[76,77] and the two protonated, positively charged sites in the salt bridge of bradykinin are both Arg, the most basic of the amino acids, but in Trp-cage one is Arg and the other is Lys. (The GBs of Arg and Lys are 1007 and 951 kJ/mol, respectively.)[63]

Solvent-exposed hydrogen-bond donor and acceptor groups can form new intramolecular hydrogen bonds upon removal of solvent,[78] thus giving rise to higher unfolding enthalpies in gas phase than in solution (Table 1). The numbers of hydrogen bonds in the 2+ and 3+ ions derived from MD simulations are plotted as a function of temperature in Figure 6. For the Q5R16 and K8R16 charge configurations of the 2+ ion the number of hydrogen bonds decreases by 1.4 and 2.4, respectively, between 302 and 445 K (Figure 6a). This corresponds to ~30 to 60 and ~50 to 100 kJ/mol, respectively, based on published hydrogen bond energies.[79,80] A direct quantitative comparison between the decrease in the calculated number of hydrogen bonds and the enthalpy change derived from model fits to the data for the 2+ ion (Table 1) is difficult because the conformational change is incomplete over this temperature range, that is, only small changes in fluorescence are measured at the highest temperatures for this charge state (Figure 2a). For the 3+ configurations, N1Q5R16 and N1K8R16, the calculated number of hydrogen bonds decreases by 2.3 and 1.9, respectively, between 302 and 445 K (Figure 6b), corresponding to ~45 to 100 and ~40 to 80 kJ/mol.[79,80] These results agree reasonably well with the values of ΔH_{int} for the 3+ N1K8R16 configuration which span the range 84 (±11) to 99 (±5) kJ/mol (Table 1). The more complete conformational change for the 3+ ion (Figure 2b) yields better model fits to the data with smaller uncertainties (Table 1) and, as a result, a more reliable comparison with calculations. Since the values of ΔH_{int} for both Trp-cage and the D9N mutant do not differ significantly and compare well with the calculated number of hydrogen bonds, the folded structures of the unsolvated ions are most likely stabilized by hydrogen bonds instead of a salt bridge. This conclusion differs from earlier estimates[26] of the energetics made prior to the mutant experiments and MD calculations of the hydrogen bonds for Trp-cage with an attached dye.

Interestingly, the values of ΔH_{int} for the N1Q5R16 configuration of the 3+ ion are higher than those of the N1K8R16 configuration (Table 1). This discrepancy occurs because the calculated change in Coulomb energy, ΔE_{Coul}, for N1Q5R16 is approximately seven times larger than that of N1K8R16. The larger ΔE_{Coul} value for N1Q5R16 is primarily due to increases in the charge−charge distances, N1−R16 and Q5−R16, which occur between 302 and 445 K during MD simulations (data not shown).

These experiments provide a unique opportunity to directly compare both the enthalpy and entropy changes of protein conformational change in solution with the values in gas phase. The enthalpy changes can be accounted for by the energies of noncovalent interactions, as demonstrated in the preceding paragraph. However, accounting for the entropy changes is more difficult. The values of ΔS for conformational change in Trp-cage are 16% to 98% higher in gas phase than in solution (Table 1). One possible contributor to the higher ΔS values in gas phase is increased order in the folded state compared to that in solution. For example, in the absence of solvent, additional local order may be induced through the solvation of charges by polar functional groups of the polypeptide backbone. The discrepancies between the solution and gas-phase ΔS values may also stem in part from the absence of ordered water[53] about the protein surface in gas phase. The free energies of transfer of individual amino acids[81] to water from organic solvents or gas phase may potentially offer a measure of water-ordering effects. However, separation of these values into their enthalpic and entropic components is hindered by enthalpy−entropy compensation.[1]

Molecular Dynamics/Fluorescence Comparison. Representative structures resulting from MD simulations of the 2+ Q5R16 and 3+ N1Q5R16 ions of Trp-cage derivatized with BODIPY TMR are shown in Figures 7 and 8, respectively, alongside the NMR structure.[38] The backbone root mean squared deviation (RMSD) from the NMR structure was calculated and averaged over all 5×10^5 structures generated during the 500 ns simulations. The RMSD values for the 2+ Q5R16 and 3+ N1Q5R16 ions at 302 K are 4.04 and 3.34 Å, respectively. At 445 K, the RMSD values for the 2+ and 3+ ions are 4.07 and 4.25 Å, respectively. Similar backbone configurations are obtained for simulated 2+ K8R16 and 3+ N1K8R16 ions shown in Figures 9 and 10, respectively. The RMSD values for the 2+ K8R16 and 3+ N1K8R16 ions at 302 K are 4.53 and 3.76 Å, respectively, and at 445 K the values are 4.74 and 3.79 Å,

(78) Kitova, E. N.; Bundle, D. R.; Klassen, J. S. *J. Am. Chem. Soc.* **2002**, *124*, 5902−5913.
(79) Grabowski, S. J. *J. Phys. Org. Chem.* **2004**, *17*, 18−31.
(80) Meot-Ner, M. *Chem. Rev.* **2005**, *105*, 213−284.
(81) Radzicka, A.; Wolfenden, R. *Biochemistry* **1988**, *27*, 1664−1670.
(82) Moser, C. C.; Keske, J. M.; Warncke, K.; Farid, R. S.; Dutton, P. L. *Nature* **1992**, *355*, 796−802.

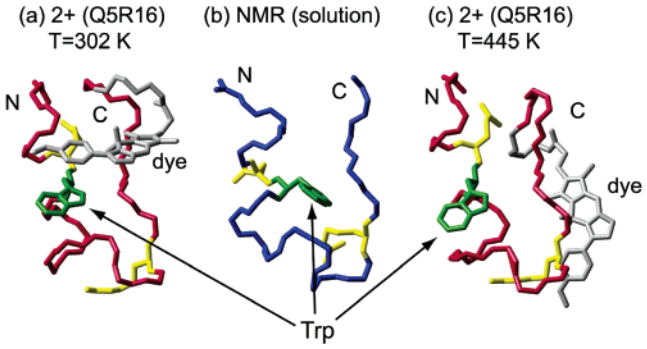

Figure 7. Representative structures resulting from simulations of the 2+ ion (Q5R16 configuration) of Trp-cage-BoTMR (red backbone) at (a) 302 K and (c) 445 K compared with (b) the native structure determined by NMR (blue backbone; ref 38). The C- and N-termini are denoted by "C" and "N", respectively, and the BoTMR dye, Trp, and charged residues are gray, green, and yellow, respectively.

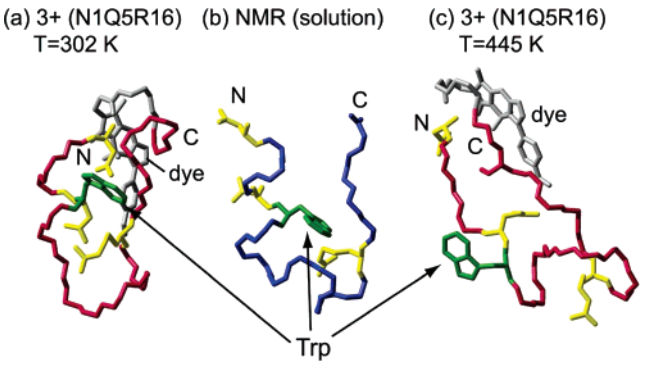

Figure 8. Representative structures resulting from simulations of the 3+ ion (N1Q5R16 configuration) of Trp-cage-BoTMR (red backbone) at (a) 302 K and (c) 445 K compared with (b) the native structure determined by NMR (blue backbone; ref 38). The BoTMR dye, Trp, and charged residues are gray, green, and yellow, respectively.

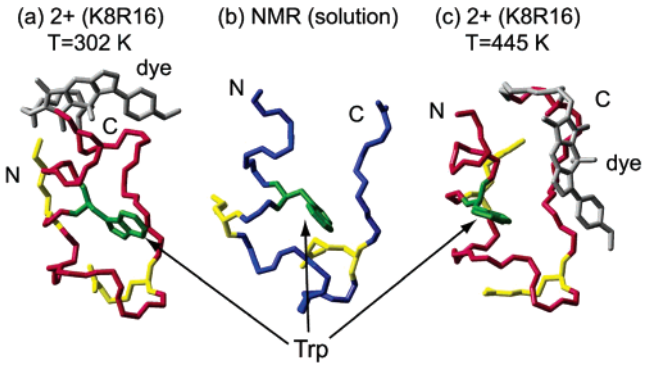

Figure 9. Representative structures resulting from simulations of the 2+ ion (K8R16 configuration) of Trp-cage-BoTMR (red backbone) at (a) 302 K and (c) 445 K compared with (b) the native structure determined by NMR (blue backbone; ref 38). The BoTMR dye, Trp, and charged residues are gray, green, and yellow, respectively.

respectively. We note that calculated structures calculated for both the Gln5 and Lys8 charge sites remain relatively compact at the higher temperature as shown in Figures 8 and 10. This is consistent with the unfolded conformations for Trp-cage in solution calculated by Pande and co-workers[42] and suggests that the fluorescence is probing the temperature dependence of the conformational fluctuations of secondary structure rather than large scale changes of the tertiary structure.

The accessible surface area (ASA) of the Trp side chain is a qualitative measure of how accessible Trp is to interactions with

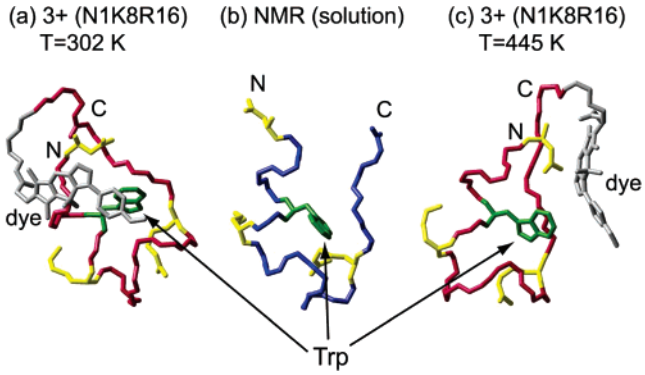

Figure 10. Representative structures resulting from simulations of the 3+ ion (N1K8R16 configuration) of Trp-cage-BoTMR (red backbone) at (a) 302 K and (c) 445 K compared with (b) the native structure determined by NMR (blue backbone; ref 38). The BoTMR dye, Trp, and charged residues are gray, green, and yellow, respectively.

molecules external to the protein. In particular, the ASA for Trp calculated from these MD simulations can indicate the propensity for quenching interactions with the attached dye. The ASA values for Trp are calculated as an average over all structures generated during the 500 ns simulation. The temperature dependence of the ASA for both charge states and configurations does not exhibit significant change over 300−445 K. Similar to the RMSD behavior, the ASA values infer relatively compact structures at all temperatures studied. The order of ASA values is N1K8R16 > K8R16 ≈ N1Q5R16 > Q5R16. Interestingly, the ASA values for configurations in which Lys8 is protonated are a factor of ∼2 larger than those in which Gln5 is protonated, for both 2+ and 3+ ions. The larger ASA values for the configurations in which Lys8 is protonated suggest that these charge configurations offer a greater probability for quenching than the configurations with protonated Gln5. The larger exposure of Trp for the protonated Lys8 configurations may be due in part to stronger Coulomb repulsion between Lys8 and Arg16 which leads to enhanced fluctuations of Trp outside the proline cage.

Quenching and Charge Effects. There is a large body of evidence[83−88] that electric fields can strongly perturb the charge-transfer process. The Coulomb fields arising from the relatively unshielded charges are large (∼10^7 to 10^8 V/cm) and could substantially alter the exothermicity of a charge-transfer reaction.[83−88] In this case, there may be optimum separations of the dye, Trp, and charged residues which lead to efficient charge transfer and quenching of the dye fluorescence. In addition to dye quenching interactions, the Coulomb fields can also have a pronounced effect on radiative absorption.[89,90] These Stark effects can cause changes in absorption by inducing spectral shifts, level splitting, and changes in the matrix element. Effects on absorption have been measured[91] for the BODIPY core molecule with external fields of ∼10^6 V/cm. Preliminary

(83) (a) Hilczer, M.; Traytak, S.; Tachiya, M. *J. Chem. Phys.* **2001**, *115*, 11249−11253. (b) Hilczer, M.; Tachiya, M. *J. Chem. Phys.* **2002**, *117*, 1759−1767.
(84) Boxer, S. G.; Goldstein, R. A.; Lockhart, D. J.; Middendorf, T. R.; Takiff, L. *J. Phys. Chem.* **1989**, *93*, 8280−8294.
(85) Lockhart, D. J.; Kirmaier, C.; Holten, D.; Boxer, S. G. *J. Phys. Chem.* **1990**, *94*, 6987−6995.
(86) Lao, K. Q.; Franzen, S.; Steffen, M.; Lambright, D.; Stanley, R.; Boxer, S. G. *Chem. Phys.* **1995**, *197*, 259−275.
(87) Tsushima, M.; Ohta, N. *J. Chem. Phys.* **2004**, *120*, 6238−6245.
(88) (a) Callis, P. R.; Liu, T. *Chem. Phys.* **2006**, *326*, 230−239. (b) Callis, P. R.; Vivian, J. T. *Chem. Phys. Lett.* **2003**, *369*, 409−414.

measurements of the dye-modified Trp-cage have observed clear evidence of temperature-dependent spectral shifts and spectral broadening. In this case, rather than an external field, the field originates on the charged residues themselves so that the conformational fluctuations are characterized by the spectral characteristics. Preliminary measurements of the fluorescence emission spectra of the 2+ and 3+ ions indicate charge state dependent spectral shifts and broadening with increasing temperature (data not shown).

As a result of these quenching and charge interactions among the residues and the dye, the underlying processes responsible for the variation in fluorescence intensity are highly dependent on the local fluctuations of the conformation. Consequently, these considerations reaffirm that these fluorescence measurements are related to the conformational fluctuations and not a static structure. Additional experiments and analysis are being pursued to help unravel these local interactions leading to the intensity variations, but the general conclusion remains clear that the fluorescence probe is sensitive to conformational fluctuations and can yield valuable information regarding biomolecule dynamics in gas phase.

Solvent Effects. Although the measured T_m of Trp-cage in 1:1 acetonitrile/water is 32 K lower than that measured in the aqueous solution without acetonitrile (Figure 3), no significant difference is observed between the melting curves of the gas-phase ions formed from these solvent systems (Figure 2). The extent to which solvent-induced changes in protein structure are retained in the gas phase is the subject of active investigation and appears to depend on the protein. Williams and co-workers[20] used BIRD to study the kinetics of heme dissociation from holomyoglobin ions formed from pseudonative (80% water/20% methanol) and denaturing (1:1 water/methanol, 0.1% acetic acid) solutions. The Arrhenius activation energies and pre-exponential factors of ions formed from denaturing solutions were lower than those of ions formed from pseudonative conditions, consistent with a retention of the solution conformation in the gas phase. Clemmer and co-workers characterized the conformations of ubiquitin ions formed from pseudonative (89% water/9% acetonitrile/2% acetic acid) and denaturing (49% water/49% acetonitrile/2% acetic acid) solutions using high-resolution ion-mobility spectroscopy.[8] The ions formed from pseudonative solutions exhibited a larger fraction of compact structures than the ions formed from denaturing solutions, providing another result which is consistent with some degree of preservation of solvent-induced conformational differences in the gas phase. However, the authors noted that the apparent correlation between solution and gas-phase structures may also stem in part from differences in the evaporative cooling of the different solvents.[8] On the other hand, Douglas and co-workers reported that the collisional cross-sections and hydrogen/deuterium exchange levels of lysozyme were essentially the same for ions formed from aqueous and denaturing (20% water/80% methanol) solutions. The authors proposed that the denatured protein refolds in the gas phase to a compact structure on the time scale of $\leq 10^{-3}$ s, thus masking the original solution-phase conformation.[11] The protein in the present study, Trp-cage, folds in only four microseconds,[40] suggesting the reasonable possibility that acetonitrile-induced changes in conformation may be reduced or eliminated owing to refolding during or after desolvation, prior to measuring fluorescence.

Conclusions

We have presented laser-induced fluorescence measurements of trapped, unsolvated ions of Trp-cage derivatized with a fluorescent dye as a means to probe temperature-induced conformational changes of the protein in a solvent-free environment. This measurement is particularly sensitive to local conformational changes which alter the interaction between the dye and a natural quencher, Trp, and, in addition, alter the distribution of Coulomb fields within the protein. A greater decrease in fluorescence is observed for the 3+ ion than for the 2+ ion between 303 and 438 K, consistent with a conformational change which is promoted by greater Coulomb repulsion in the higher charge state. The dependence on charge state is supported by MD simulations which indicate compact conformations and a markedly greater value for Trp accessibility (ASA) for the 3+ ion than for the 2+ ion. MD calculations of Trp accessibility for ions in which Lys8 is charged appear to be more consistent with the experimental data than those in which Gln5 is charged. Although replacing Asp9 with Asn clearly disrupts the Trp-cage fold in solution, this substitution results in only slight changes in the melting curves of the unsolvated ions. This suggests that a + − + salt bridge involving Lys8, Asp9, and Arg16 is important for stabilizing the fold in solution but does not significantly contribute to the stability of the unsolvated ions. The experimentally derived enthalpy change of unsolvated ions can be accounted for by the decrease in the number of hydrogen bonds with increasing temperature indicated by MD simulations. MD calculations for the temperature dependence of hydrogen bonds in the 3+ charge state in which Lys8 is charged appear to be more consistent with the experimental data than those in which Gln5 is charged. The uncertainty in the experimental thermochemical values for the 2+ ion precludes a reliable conclusion for this charge state. A planned analysis of Coulomb field effects should help to assign the charge sites with greater certainty. MD simulations suggest that conformational fluctuations are the important dynamical behavior leading to the changes in fluorescence. The melting curves of the unsolvated Trp-cage ions are invariant with the acetonitrile concentration of the electrospray solution, possibly as a result of protein refolding during or after desolvation. Strong Coulomb fields arising from the unshielded charges can affect the measured fluorescence through (1) shifts and/or broadening of the absorption spectra owing to Stark effects and (2) alterations of the exothermicity of charge-transfer processes. Extension of these studies to time-resolved measurements of the dye lifetime will help to isolate the quenching interaction of the dye by Trp and possibly provide a finer comparison with local dynamics characterized by MD simulations. It is clear that defining the mechanisms of the local interactions in gas-phase biomolecules requires more study. However, an essential result of the measurements reported here is that the fluorescence probe yields a consistent, physical picture of biomolecule dynamics evolving with temperature. This work lays the foundation for using fluorescence measurements combined with theoretical calculations to probe the individual interactions which stabilize higher order structure of biomol-

(89) Liptay, W. In *Electronic States*; Lim, E. C., Ed.; Academic Press: 1974; Vol. 1, p 129.
(90) Bublitz, G. U.; Boxer, S. G. *Annu. Rev. Phys. Chem.* **1997**, *48*, 213−242.
(91) Bergström, F.; Mikhalyov, I.; Hägglöf, P.; Wortmann, R.; Ny, T.; Johansson, L. B.-Å. *J. Am. Chem. Soc.* **2002**, *124*, 196−204.

ecules and noncovalent complexes in the absence of the complicating effects of solvent.

Acknowledgment. The authors thank Jan Meinen and Susanne Schulze for solution measurements and Abraham Szöke for useful discussions. This work was supported by the Rowland Institute at Harvard.

Supporting Information Available: Complete ref 59, MD force field parameters for dye, data for BoTR-derivatized Trp-cage ions. This material is available free of charge via the Internet at http://pubs.acs.org.

JA065092S